

inhibitory potency of physostigmine in HLM was stronger than that in HJM. The K_i value of manidipine in HJC was lower than that in RJM or RJC.

DISCUSSION

In multiple drug therapy, drug interactions are important issues that must be taken into consideration. It is possible that co-administration of several drugs can change the efficacy of a drug due to the inhibition of drug-metabolizing enzymes. Investigations of inhibitory effects for CES activity would provide useful information for the prediction of *in vivo* drug interactions and for drug development. In the present study, we investigated the inhibitory effects on hydrolysis of two prodrugs in human and rat in order to clarify the species differences in CES inhibition. Imidapril and CPT-11 were used as representative CES1 and CES2 substrates.

In imidaprilat formation from imidapril by CES1, delapril and temocapril were inhibited weakly (>50% of control) in human liver, whereas they showed more than 90% inhibition in rat liver (Fig. 1). Human CES1 was shown to be less efficient at catalysis of bulky substrates than rabbit CES because of the size-limited access of substrates to the active site (Wadkins et al., 2001). Since delapril and temocapril are substrates of human CES1 (Takai et al., 1997) and are more bulky than imidapril, size differences of the active site between human and rat may have contributed to the present results.

Dexamethasone and docetaxel, which are not CES substrates, inhibited the imidaprilat formation weakly in human liver (Fig. 1). The two drugs exhibited weak inhibitions for the hydrolysis of 4-methylumbelliferyl acetate catalyzed by both CES1A1 and CES2 ($IC_{50} > 0.7$ mM) (Quinney et al., 2005), consistent with our results. As shown in Table 1, the imidaprilat formation in HLM was inhibited competitively by procainamide. Bailey

and Briggs (2003) suggested that procainamide inhibits human CES1. Procainamide is also known as a choline binding pocket-specific inhibitor (Jaganathan and Boopathy, 1998) and has been reported to inhibit human butyrylcholinesterase competitively ($K_i = 9 \mu\text{M}$) (Rush et al., 1981). Because the amino acid sequences at the active site were highly conserved among esterase B, which is inhibited by organophosphorus compounds such as CES and butyrylcholinesterase (Satoh and Hosokawa, 1995), it is reasonable to assume that procainamide inhibits CES1 activity. Imidaprilat formations in rat liver were inhibited more strongly by NDGA than in human liver (Table 1). NDGA is known as a potent CES inhibitor (Schegg and Welch, 1984). These inhibition patterns showed uncompetitive inhibition except RJM, suggesting that NDGA could bind to a site different from the active site. Actually, human CES1 has ligand binding sites other than the active site and each site is called a side door and a Z-site (Bencharit et al., 2003b). Rat CES isoforms may contain such other sites as human CES1. The inhibitory potencies of carvedilol were stronger in rat liver and jejunum than in human liver (Table 1). Although the structures of rat CES isoforms have not been revealed, structural differences between human and rat CES may be involved in the species differences of the inhibition potency.

The inhibitory effects in both microsomes and cytosol showed similar tendencies in imidaprilat formations in human and rat in the present study. The activities in microsomes were more than 2-fold higher than those in cytosol. However, taking the total protein content into consideration, 1:5, the contribution of cytosolic CES is as important as microsomal CES (Tabata et al., 2004). Thus, CES inhibition in the cytosol should be taken into consideration as well as in microsomes.

The SN-38 formations in jejunum were inhibited more strongly by manidipine than in liver in the present study. Manidipine is similar in structure to nifedipine and has larger

alcohol groups that are hydrolyzed well by CES2. Since nifedipine did not inhibit SN-38 formation in HJC, manidipine could be a potent CES2 inhibitor in human jejunum. Carvedilol also showed inhibitions for the SN-38 formations in both human liver and jejunum except HJM, whereas there were no inhibitions in rat liver and jejunum, indicating species differences in CES2 activity. As shown in Figs. 1 and 2, the SN-38 formations in all enzyme sources were not inhibited by procainamide, whereas the imidaprilat formations were inhibited strongly. The major isoforms involved in the hydrolysis of CPT-11 and imidapril are CES2 and CES1, respectively (Schwer et al., 1997; Takai et al., 1997). Human CES1 is also expressed in liver at much higher levels than in small intestine (Imai, 2006), whereas CES2 is abundant in small intestine (Schwer et al., 1997). Thus, procainamide exhibited more potent inhibitory effects for CES1 than for CES2.

Because there were no drugs and compounds that inhibited the SN-38 formations potently in rat liver, the K_i values in RLM and RLC were not determined. On the other hand, the SN-38 formations in RJM and RJC were inhibited competitively by manidipine with low K_i values, suggesting that tissue differences would exist in the inhibition of CPT-11 hydrolase activity. Satoh et al. (1994) demonstrated that ES-4 and ES-10 purified from RLM, which both belong to CES1 family, have the ability to hydrolyze CPT-11 more effectively than human CES1. By Northern blot analysis, both CES1 and CES2 were expressed in rat liver (Sanghani et al., 2002), whereas CES2 isoforms were mainly expressed in Wistar rat jejunum, but the mRNA expression levels of the CES1 isoforms were much lower than those of CES2 (Masaki et al., 2007). From these studies, it could be speculated that CES2 isoforms are responsible for CPT-11 hydrolysis, thus the potent inhibitory effects by manidipine may be the result of CES2 inhibition in rat jejunum.

Although the clinical serum concentration of manidipine is in the nM order, intestinal mucosa may be exposed to high concentrations of a given drug. Therefore, we have to keep the CES2 inhibition in mind in clinical practice. Manidipine also exhibited potent competitive inhibition in HJC, whereas imidaprilat formations in human liver were not inhibited. The entrance to the active site of human CES1 is smaller than CES2 (Wadkins et al., 2001), leading to the difference in inhibition. Although crystal structure of human CES2 is not obvious, human CES2 contains *N*-glycosylation sites at two positions whereas CES1 has one *N*-glycosylation site (Bencharit et al., 2003a).

In the present study, the K_i values of physostigmine, a specific cholinesterase inhibitor, were approximately 10-fold lower in HLM ($K_i = 0.2 \pm 0.0 \mu\text{M}$) and HJC ($K_i = 0.3 \pm 0.0 \mu\text{M}$) than the other enzyme sources. These K_i values were close to the previous result that physostigmine inhibited the hydrolysis of 4-methylumbelliferyl acetate by purified human CES2 ($K_i = 0.10 \pm 0.01 \mu\text{M}$) (Pindel et al., 1997). CES1 and CES2 family share 40–50% amino acid sequence identity but the substrate specificities of CES1 and CES2 in human are different; CES1 hydrolyzes compounds with larger acyl groups and CES2 preferentially hydrolyzes large alcohol groups (Sato et al., 2002; Imai, 2006).

The present comprehensive study clarified that species differences existed in the inhibition of imidapril and CPT-11 hydrolysis. The present study should provide useful information on the differences in CES activity in human and rat.

Acknowledgements. We acknowledge Mitsubishi Tanabe Pharma Corporation for kindly providing imidapril and imidaprilat and Takeda Pharmaceutical Company for kindly supplying delapril. We thank Mr. Brent Bell for reviewing the manuscript.

References

- Bailey DN and Briggs JR (2003) Procainamide and quinidine inhibition of the human hepatic degradation of meperidine in vitro. *J Anal Toxicol* **27**:142-144.
- Bencharit S, Morton CL, Hyatt JL, Kuhn P, Danks MK, Potter PM, Redinbo MR (2003a) Crystal structure of human carboxylesterase 1 complexed with the Alzheimer's drug tacrine: from binding promiscuity to selective inhibition. *Chem Biol* **10**:341-349.
- Bencharit S, Morton CL, Xue Y, Potter PM, and Redinbo MR (2003b) Structural basis of heroin and cocaine metabolism by a promiscuous human drug-processing enzyme. *Nat Struct Biol* **10**:349-356.
- Buratti FM and Testai E (2005) Malathion detoxification by human hepatic carboxylesterases and its inhibition by isomalathion and other pesticides. *J Biochem Mol Toxicol* **19**:406-414.
- Emoto C, Yamazaki H, Iketaki H, Yamasaki S, Satoh T, Shimizu R, Suzuki S, Shimada N, Nakajima M, and Yokoi T (2001) Cooperativity of α -naphthoflavone in cytochrome P450 3A-dependent drug oxidation activities in hepatic and intestinal microsomes from mouse and human. *Xenobiotica* **31**:265-275.
- Fleming CD, Bencharit S, Edwards CC, Hyatt JL, Tsurkan L, Bai F, Fraga C, Morton CL, Howard-Williams EL, Potter PM, and Redinbo MR (2005) Structural insights into drug processing by human carboxylesterase 1: tamoxifen, mevastatin, and inhibition by benzil. *J Mol Biol* **352**:165-177.
- Humerickhouse R, Lohrbach K, Li L, Bosron WF, and Dolan ME (2000) Characterization of CPT-11 hydrolysis by human liver carboxylesterase isoforms hCE-1 and hCE-2. *Cancer Res* **60**:1189-1192.
- Imai T (2006) Human carboxylesterase isozymes: catalytic properties and rational drug

- design. *Drug Metab Pharmacokinet* **21**:173-185.
- Jaganathan L and Boopathy R (1998) Interaction of Triton X-100 with acyl pocket of butyrylcholinesterase: effect on esterase activity and inhibitor sensitivity of the enzyme. *Indian J Biochem Biophys* **35**:142-147.
- Linke T, Dawson H, and Harrison EH (2005) Isolation and characterization of a microsomal acid retinyl ester hydrolase. *J Biol Chem* **280**:23287-23294.
- Masaki K, Hashimoto M, and Imai T (2007) Intestinal first-pass metabolism via carboxylesterase in rat jejunum and ileum. *Drug Metab Dispos* **35**:1089-1095.
- Mésange F, Sebbar M, Capdevielle J, Guillemot JC, Ferrara P, Bayard F, Poirot M, and Faye JC (2002) Identification of two tamoxifen target proteins by photolabeling with 4-(2-morpholinoethoxy)benzophenone. *Bioconjug Chem* **13**:766-772.
- Murakami K, Takagi Y, Mihara K, and Omura T (1993) An isozyme of microsomal carboxyesterases, carboxyesterase Sec, is secreted from rat liver into the blood. *J Biochem* **113**:61-66.
- Pindel EV, Kedishvili NY, Abraham TL, Brzezinski MR, Zhang J, Dean RA, and Bosron WF (1997) Purification and cloning of a broad substrate specificity human liver carboxylesterase that catalyzes the hydrolysis of cocaine and heroin. *J Biol Chem* **272**:14769-14775.
- Quinney SK, Sanghani SP, Davis WI, Hurley TD, Sun Z, Murry DJ, and Bosron WF (2005) Hydrolysis of capecitabine to 5'-deoxy-5-fluorocytidine by human carboxylesterases and inhibition by loperamide. *J Pharmacol Exp Ther* **313**:1011-1016.
- Rush RS, Main AR, Kilpatrick BF, and Faulkner GD (1981) Inhibition of two monomeric butyrylcholinesterases from rabbit liver by chlorpromazine and other drugs. *J*

Pharmacol Exp Ther **216**:586-591.

Sanghani SP, Davis WI, Dumaul NG, Mahrenholz A, and Bosron WF (2002)

Identification of microsomal rat liver carboxylesterases and their activity with retinyl palmitate. *Eur J Biochem* **269**:4387-4398.

Sanghani SP, Quinney SK, Fredenburg TB, Davis WI, Murry DJ, and Bosron WF (2004)

Hydrolysis of irinotecan and its oxidative metabolites, 7-ethyl-10-[4-*N*-(5-aminopentanoic acid)-1-piperidino] carbonyloxycamptothecin and 7-ethyl-10-[4-(1-piperidino)-1-amino]-carbonyloxycamptothecin, by human carboxylesterases CES1A1, CES2, and a newly expressed carboxylesterase isoenzyme, CES3. *Drug Metab Dispos* **32**:505-511.

Satoh T and Hosokawa M (1995) Molecular aspects of carboxylesterase isoforms in

comparison with other esterases. *Toxicol Lett* **82-83**:439-445.

Satoh T, Hosokawa M, Atsumi R, Suzuki W, Hokusui H, and Nagai E (1994) Metabolic

activation of CPT-11, 7-ethyl-10-[4-(1-piperidino)-1-piperidino]carbonyloxycamptothecin, a novel antitumor agent, by carboxylesterase. *Biol Pharm Bull* **17**:662-664.

Satoh T, Taylor P, Bosron WF, Sanghani SP, Hosokawa M, and La Du BN (2002) Current

progress on esterases: from molecular structure to function. *Drug Metab Dispos* **30**:488-493.

Schegg KM and Welch W Jr (1984) The effect of nordihydroguaiaretic acid and related

lignans on formyltetrahydrofolate synthetase and carboxylesterase. *Biochim Biophys Acta* **788**:167-180.

Schwer H, Langmann T, Daig R, Becker A, Aslanidis C, and Schmitz G (1997)

Molecular cloning and characterization of a novel putative carboxylesterase, present

- in human intestine and liver. *Biochem Biophys Res Commun* **233**:117-120.
- Tabata T, Katoh M, Tokudome S, Nakajima M, and Yokoi T (2004) Identification of the cytosolic carboxylesterase catalyzing the 5'-deoxy-5-fluorocytidine formation from capecitabine in human liver. *Drug Metab Dispos* **32**:1103-1110.
- Takahashi S, Katoh M, Saitoh T, Nakajima M, and Yokoi T (2008) Allosteric kinetics of human carboxylesterase 1: Species differences and interindividual variability. *J Pharm Sci* **97**:5434-5445.
- Takai S, Matsuda A, Usami Y, Adachi T, Sugiyama T, Katagiri Y, Tatematsu M, and Hirano K (1997) Hydrolytic profile for ester- or amide-linkage by carboxylesterases pI 5.3 and 4.5 from human liver. *Biol Pharm Bull* **20**:869-873.
- Wadkins RM, Hyatt JL, Edwards CC, Tsurkan L, Redinbo MR, Wheelock CE, Jones PD, Hammock BD, and Potter PM (2007) Analysis of mammalian carboxylesterase inhibition by trifluoromethylketone-containing compounds. *Mol Pharmacol* **71**:713-723.
- Wadkins RM, Morton CL, Weeks JK, Oliver L, Wierdl M, Danks MK, and Potter PM (2001) Structural constraints affect the metabolism of 7-ethyl-10-[4-(1-piperidino)-1-piperidino]carbonyloxycamptothecin (CPT-11) by carboxylesterases. *Mol Pharmacol* **60**:355-362.

Footnotes

Send reprint requests to: Tsuyoshi Yokoi, Ph.D. Faculty of Pharmaceutical Sciences,
Kanazawa University, Kakuma-machi, Kanazawa 920-1192, Japan. E-mail:
tyokoi@kenroku.kanazawa-u.ac.jp

¹S.T. and M.K. contributed equally to this work.

²Present address: Miki Katoh, Ph.D. Faculty of Pharmacy, Meijo University, 150
Yagotoyama, Tempaku-ku, Nagoya 468-8503, Japan.

Legends for Figures

FIG. 1. Inhibitory effect of 15 drugs and one compound on imidaprilat formation catalyzed by HLM and HLC (A), RLM and RLC (B), and RJM and RJC (C). The concentrations of imidapril and the 15 drugs and one compound were 150 and 300 μM except for manidipine (50 μM), respectively. Each column represents the mean of duplicate determinations. The control activity was 0.4 nmol/min/mg protein in HLM, 0.05 nmol/min/mg protein in HLC, 37.6 nmol/min/mg protein in RLM, 17.6 nmol/min/mg protein in RLC, 0.8 nmol/min/mg protein in RJM, and 0.4 nmol/min/mg protein in RJC. ND, not detected.

FIG. 2. Inhibitory effect of 15 drugs and one compound on SN-38 formation catalyzed by HLM and HLC (A), HJM and HJC (B), RLM and RLC (C), and RJM and RJC (D). The concentrations of CPT-11 and the 15 drugs and one compound were 5 and 10 μM , respectively. Each column represents the mean of duplicate determinations. The control activity was 3.7 pmol/min/mg protein in HLM, 0.9 pmol/min/mg protein in HLC, 0.6 pmol/min/mg protein in HJM, 6.5 pmol/min/mg protein in HJC, 5.1 pmol/min/mg protein in RLM, 2.3 pmol/min/mg protein in RLC, 13.5 pmol/min/mg protein in RJM, and 4.6 pmol/min/mg protein in RJC. NA, not available.

FIG. 3. Inhibitory effect of imidaprilat formation by procainamide (A), carvedilol (B), and NDGA (C) and SN-38 formation by carvedilol (D), manidipine (E), and physostigmine (F). A and D, HLM; B, RLC; C, RJC; E, HJC; F, RJM. Each point represents the mean of duplicate determinations. The control activity was the same as that in Figs. 1 and 2.

Table 1. The K_i values and inhibition types for the imidaprilat formation.

Enzyme source	Inhibitor	K_i μM	Inhibition type
HLM	NDGA	13.3 ± 1.5	Mixed
	Procainamide	29.3 ± 4.8	Competitive
HLC	NDGA	2.9 ± 0.5	Uncompetitive
	Procainamide	34.5 ± 2.2	Competitive
RLM	Carvedilol	1.6 ± 0.2	Competitive
	NDGA	0.4 ± 0.0	Uncompetitive
RLC	Carvedilol	2.3 ± 0.3	Mixed
	NDGA	0.4 ± 0.0	Uncompetitive
RJM	Carvedilol	8.8 ± 0.5	Competitive
	NDGA	11.0 ± 2.2	Mixed
RJC	Carvedilol	5.1 ± 1.0	Competitive
	NDGA	3.2 ± 0.3	Uncompetitive

Data generated by nonlinear regression analysis are expressed as mean \pm SE.

The concentrations of imidaprilat ranged from 100 to 500 μM for HLM and HLC, from 25 to 150 μM for RLM, from 15 to 90 μM for RLC, from 20 to 80 μM for RJM, and from 25 to 100 μM for RJC. The concentrations of inhibitors ranged as follow: carvedilol, 1-6 μM for RLM, 1-6 μM for RLC, 4-24 μM for RJM, and 5-30 μM for RJC; NDGA, 10-40 μM for HLM, 2-7 μM for HLC, 0.2-2 μM for RLM, 0.2-1.5 μM for RLC, 3-15 μM for RJM, and 2-12 μM for RJC; procainamide, 25-150 μM for HLM and 25-100 μM for HLC.

Table 2. The K_i values and inhibition types for the SN-38 formation.

Enzyme source	Inhibitor	K_i μM	Inhibition type
HLM	Carvedilol	1.6 ± 0.2	Competitive
	Physostigmine	0.2 ± 0.0	Competitive
HLC	Carvedilol	4.1 ± 0.3	Competitive
	Physostigmine	1.6 ± 0.3	Competitive
HJM	Physostigmine	3.1 ± 0.2	Noncompetitive
HJC	Manidipine	0.1 ± 0.0	Competitive
	Physostigmine	0.3 ± 0.0	Mixed
RJM	Manidipine	0.8 ± 0.1	Competitive
	Physostigmine	2.5 ± 0.3	Mixed
RJC	Manidipine	0.6 ± 0.1	Competitive
	Physostigmine	3.1 ± 0.4	Mixed

Data generated by nonlinear regression analysis are expressed as mean \pm SE.

The concentrations of CPT-11 ranged from 2.5 to 15 μM for all enzyme sources.

The concentrations of the inhibitors ranged as follow: carvedilol, 2-8 μM for HLM and 1-12 μM for HLC; manidipine, 0.1-0.5 μM for HJC, 0.5-5 μM for RJM, and 0.5-4 μM for RJC; physostigmine, 0.1-0.6 μM for HLM, 0.2-5 μM for HLC, 1-6 μM for HJM, 0.2-1 μM for HJC, 1-8 μM for RJM, and 2-10 μM for RJC.

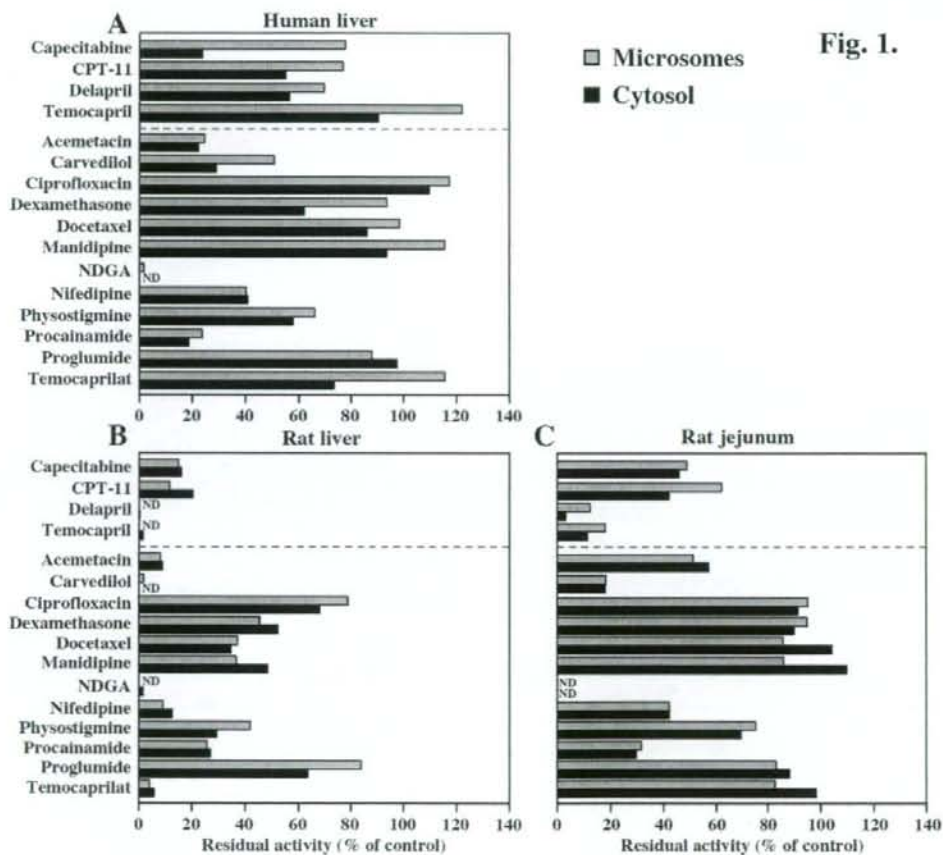
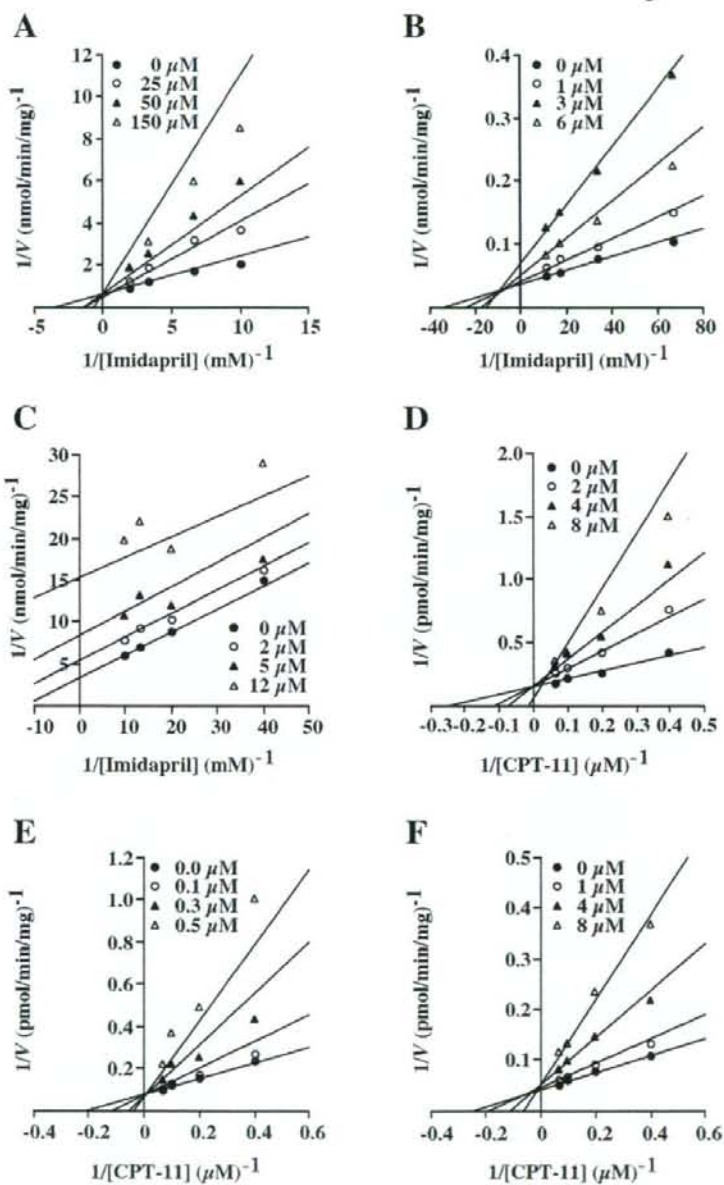


Fig. 3.



MicroRNA regulates human vitamin D receptor

Takuya Mohri, Miki Nakajima, Shingo Takagi, Sayaka Komagata & Tsuyoshi Yokoi

Drug Metabolism and Toxicology, Faculty of Pharmaceutical Sciences, Kanazawa University,
Kakuma-machi, Kanazawa 920-1192, Japan

Short title: MicroRNA regulates human VDR

Key words: microRNA; VDR; post-transcriptional regulation

Journal category: Cancer Cell Biology

To whom all correspondence should be addressed:

Tsuyoshi Yokoi, Ph.D.,
Drug Metabolism and Toxicology
Faculty of Pharmaceutical Sciences
Kanazawa University
Kakuma-machi
Kanazawa 920-1192, Japan
Tel / Fax +81-76-234-4407
E-mail: tyokoi@kenroku.kanazawa-u.ac.jp

Abbreviations: VDR, vitamin D receptor; miRNA, microRNA; MRE125b, miR-125b recognition element; $1,25(\text{OH})_2\text{D}_3$, $1\alpha,25$ -Dihydroxyvitamin D_3 ; RXR, retinoid X receptor; VDRE, vitamin D responsive elements; 3'-UTR, 3'-untranslated region; AsO, antisense LNA/DNA mixed oligonucleotides; ER, estrogen receptor; PXR, pregnane X receptor.

Novelty and impact of this paper: We found that human VDR is post-transcriptionally regulated by microRNA. The down-regulation of miR-125b in cancer may result in the up-regulation of VDR and augmentation of the anti-tumor effects of $1,25(\text{OH})_2\text{D}_3$.

Abstract

Most of the biological effects of $1\alpha,25$ -dihydroxyvitamin D_3 ($1,25(OH)_2D_3$) are elicited by the binding to vitamin D receptor (VDR), which regulates gene expression. Earlier studies reported no correlation between the VDR protein and mRNA levels, suggesting the involvement of post-transcriptional regulation. MicroRNAs (miRNAs) are small non-coding RNAs that regulate gene expression through translational repression or mRNA degradation. A potential miR-125b recognition element (MRE125b) was identified in the 3'-untranslated region of human VDR mRNA. We investigated whether VDR is regulated by miR-125b. In luciferase assays using a plasmid containing the MRE125b, the antisense oligonucleotide for miR-125b significantly increased (130% of control) the reporter activity in KGN cells, whereas the precursor for miR-125b significantly decreased (40% of control) the reporter activity in MCF-7 cells, suggesting that miR-125b functionally recognized the MRE125b. By electrophoretic mobility shift assays, it was demonstrated that the overexpression of miR-125b significantly decreased the endogenous VDR protein level in MCF-7 cells to 40% of control. $1,25(OH)_2D_3$ drastically induced the CYP24 mRNA level in MCF-7 cells, but the induction was markedly attenuated by the overexpression of miR-125b. In addition, the anti-proliferative effects of $1,25(OH)_2D_3$ in MCF-7 cells were significantly abolished by the overexpression of miR-125b. These results suggest that the endogenous VDR level was repressed by miR-125b. In conclusion, we found that miR-125b post-transcriptionally regulated human VDR. Since the miR-125b level is known to be down-regulated in cancer, such a decrease may result in the up-regulation of VDR in cancer and augmentation of the anti-tumor effects of $1,25(OH)_2D_3$.

Introduction

1
2
3
4
5
6
7
8
9
10
11
12
13
14
15
16
17
18
19
20
21
22
23
24
25
26
27
28
29
30
31
32
33
34
35
36
37
38
39
40
41
42
43
44
45
46
47
48
49
50
51
52
53
54
55
56
57
58
59
60

$1\alpha,25$ -Dihydroxyvitamin D₃ (1,25(OH)₂D₃ or calcitriol), a biologically active metabolite of vitamin D₃, is known as a classical regulator of calcium and bone homeostasis.^{1,2} Vitamin D deficiency is linked to rickets and osteoporosis.³ Over the last 25 years, additional roles have been found for vitamin D in the regulation of cell processes such as cell growth, differentiation and apoptosis. Accumulating evidence has revealed that vitamin D deficiency is also associated with the risk of cancer.⁴ Since the vitamin D system has relevance for both the prevention and treatment of cancer,³ the development of a number of novel synthetic vitamin D analogues as a therapeutic agent in cancer has been attempted.

Most of the biological effects of 1,25(OH)₂D₃ are elicited by the binding to vitamin D receptor (VDR; NR1I1),⁵ which belongs to the superfamily of nuclear steroid hormone receptors. After ligand binding, the VDR forms a heterodimer with retinoid X receptor (RXR; NR2B1) and binds to vitamin D responsive element (VDRE) in the regulatory region of the target genes.⁶ The VDR is expressed not only in the classical vitamin D responsive organs including the intestine, bone and kidney but also in many other nonclassical vitamin D responsive organs including the liver, suggesting a broader role of the receptor.⁷ It has been reported that, at the protein level, the VDR expression is higher in breast⁸ and thyroid⁹ cancers than in normal tissues, but no obvious difference was found in cancer and normal tissues at the mRNA level. In colon cancer, the VDR mRNA and protein expression levels are gradually increased in the early stages of carcinogenesis, but the VDR mRNA decreases subsequently to lower levels during advancement.¹⁰ Thus, the VDR expression is up-regulated in cancers, although the expression levels seem to change during disease progression and in response to therapies. However, the mechanism of the up-regulation of VDR protein in cancer has not been clarified. One clue is that there is no correlation between the VDR protein and mRNA levels, suggesting the involvement of post-transcriptional regulation.

To uncover the molecular mechanism of the post-transcriptional regulation, we sought to determine whether microRNA (miRNA) might be involved in the regulation of VDR.

1
2
3
4 MiRNAs are an evolutionarily conserved class of endogenous ~22-nucleotide non-coding
5 RNAs, and play a key role in diverse biological processes, including development, cell
6 proliferation, differentiation, apoptosis, and cancer initiation and progression.¹¹⁻¹³ MiRNAs
7 recognize the 3'-untranslated region (3'-UTR) of the target mRNA and cause translational
8 repression or mRNA degradation.¹⁴ To date, approximately 700 miRNAs have been identified
9 in human, and more than one-third of all human genes have been predicted to be miRNA
10 targets.¹⁵ The expression of global miRNAs is deregulated in most types of human cancers.¹³
11 In the present study, we investigated the potential involvement of miRNAs in the
12 post-transcriptional regulation of human VDR expression.
13
14
15
16
17
18
19
20
21
22
23
24

25 **Materials and Methods**

26 *Chemicals and reagents*

27
28
29
30 1,25(OH)₂D₃ and corticosterone were purchased from Wako Pure Chemical Industries
31 (Osaka, Japan). The pGL3-promoter vector, phRL-TK plasmid, pT7Blue T-Vector, and a
32 dual-luciferase reporter assay system were purchased from Promega (Madison, WI).
33 LipofectAMINE2000 and LipofectAMINE RNAiMAX were from Invitrogen (Carlsbad, CA).
34 Pre-miR miRNA Precursors for miR-125b-1 and negative control #2 were from Ambion
35 (Austin, TX). Antisense LNA/DNA mixed oligonucleotides (AsO) for miR-125b
36 (5'-TCACAAGTTAGGGTCTCAGGGA-3', underlined letters are LNA) and for negative
37 control (5'-AGACTAGCGGTATCTTAAACC-3') were from Greiner Japan (Tokyo, Japan).
38 All primers and oligonucleotides were commercially synthesized at Hokkaido System
39 Sciences (Sapporo, Japan). Antibodies to VDR (C-20) and RXR α (D-20) were from Santa
40 Cruz Biotechnology (Santa Cruz, CA). Restriction enzymes were from Takara (Shiga, Japan),
41 TOYOBO (Osaka, Japan), and New England Biolabs (Beverly, MA). All other chemicals and
42 solvents were of the highest grade commercially available.
43
44
45
46
47
48
49
50
51
52
53
54
55
56
57
58
59
60

Cells and culture conditions

1
2
3
4 The human breast adenocarcinoma cell lines MCF-7 and MDA-MB-435, the human
5 colon carcinoma cell lines LS180, and the human embryonic kidney cell line HEK293 were
6 obtained from the American Type Culture Collection (Rockville, MD). The human ovarian
7 granulosa-like tumor cell line KGN¹⁶ and the human hepatoma cell line HepG2 were obtained
8 from Riken Gene Bank (Tsukuba, Japan). MCF-7 cells and LS180 cells were cultured in
9 Dulbecco's modified Eagle's medium (DMEM) (Nissui Pharmaceutical, Tokyo, Japan)
10 supplemented with 0.1 mmol/L nonessential amino acid (Invitrogen) and 10% fetal bovine
11 serum (FBS) (Invitrogen). MDA-MB-435 cells and HepG2 cells were cultured in DMEM
12 supplemented with 10% FBS. HEK293 cells were cultured in DMEM supplemented with 4.5
13 g/L glucose, 10 mmol/L HEPES, and 10% FBS. KGN cells were cultured in a 1:1 mixture of
14 DMEM and Ham's F-12 medium (Nissui Pharmaceutical) supplemented with 10% FBS.
15
16
17
18
19
20
21
22
23
24
25
26
27
28 These cells were maintained at 37°C under an atmosphere of 5% CO₂-95% air.
29
30
31

32 *Real-time RT-PCR for mature miR-125b*

33
34 For the quantification of mature miR-125b, polyadenylation and reverse transcription
35 were performed using an NCode miRNA First-Strand cDNA Synthesis Kit (Invitrogen)
36 according to the manufacturer's protocol. The forward primer for miR-125b was 5'-TCC CTG
37 AGA CCC TAA CTT GTG A-3', and the reverse primer was the supplemented universal
38 qPCR primer. The real-time PCR was performed using a Smart Cycler (Cepheid, Sunnyvale,
39 CA) with Smart Cycler software (version 1.2b) as follows. After an initial denaturation at
40 95°C for 30 s, the amplification was performed by denaturation at 95°C for 10 s, annealing and
41 extension at 60°C for 10 s for 45 cycles.
42
43
44
45
46
47
48
49
50
51

52 *Construction of reporter plasmids*

53
54 To construct luciferase reporter plasmids, various target fragments were inserted into the
55 XbaI site, downstream of the luciferase gene in the pGL3-promoter vector. The sequence from
56 +1786 to +1813 in the human VDR mRNA (5'-CAG GAG AAA TGC ATC CAT TCC TCA
57 GGG A-3') was termed the miR-125b recognition element (MRE125b). The region from
58
59
60